DESIGN OF FURNACE HEAD TEMPERATURE CONTROL SYSTEM DESIGN FOR 3D PRINTER USING FUZZY LOGIC CONTROLLER

Thanh-Lam Bui[1,*], Van-Truong Nguyen[1], Dinh-Hieu Phan[1], Duc-Quang Nguyen[1], Hoang-Anh Do[1], Minh-Thuan Le[1], Van-Tu Phung[1]

DOI: http://doi.org/ 10.57001/huih5804.2025.264

ABSTRACT

Temperature control is an important factor that helps ensure high quality in 3D printing. Traditional controllers often struggle to handle the nonlinear characteristics, and time delays inherent in heating systems on 3D printers. This study proposes a translucent controller (FLC) to improve the ability to regulate the temperature in 3D printers. FLC with its ability to handle language variables and uncertain information, provides a powerful alternative to traditional control methods. FLC is designed to control the nozzle temperature of 3D printers using filament technology. Simulation and experimental results show that FLC is superior to traditional PID controllers in minimizing overheating, steady state error and fast response time. In addition, FLC's ability to adapt to different printing conditions ensures stability and efficiency in temperature regulation, suitable for a wide range of materials and printing environments. The study shows the control potential of unstable systems using FLC, contributing to improving the efficiency and reliability of production systems.

Keywords: *Temperature control, 3D printer, fuzzy logic controller.*

[1]School of Mechanical and Automotive Engineering, Hanoi University of Industry, Vietnam

[*]Email: thanhlam710@gmail.com

Received: 13/3/2025

Revised: 02/5/2025

Accepted: 25/7/2025

1. INTRODUCTION

Rapid prototyping [1], customized manufacture, and optimal material use are just a few of the remarkable advantages that the advancement of 3D printing technology has brought about in the automated manufacturing sector. The need for high-quality 3D printed goods is growing, making exact control over operating parameters particularly temperature essential. Particularly in 3D printing systems that use plastic fiber materials, temperature is thought to be a determining factor in the quality of printed goods [2]. Uncontrolled temperature changes [3] can cause raw materials to distort, delainate, or distribute unevenly, which will impair the product's mechanical qualities and appearance [4]. To guarantee effective material melting and distribution in plastic fiber 3D printing systems, the nozzle temperature must be accurately controlled [5]. Due to the nonlinear nature [6], latency, and the impact of extraneous interference, this poses significant issues. Despite being widely utilized because of their ease of use and effectiveness in linear contexts, traditional controllers like PIDs have considerably worse performance when dealing with nonlinear characteristics and changes in operating conditions. Consequently, there was an immediate demand for sophisticated and flexible control techniques [7].

An enhanced control technique that can manage nonlinear properties and perturbations in systems is the fuzzy logic controller (FLC) [8]. In contrast to conventional control techniques that rely on rigid mathematical models, FLC models complex and unpredictable systems using fuzzy inference and language rules [9]. The flexibility and adaptability of FLC make it especially well-suited for temperature control in 3D printers, where nonlinear characteristics and external influences are significant.

The use of a fuzzy logic controller (FLC) to regulate the temperature in 3D printers made of plastic fiber is investigated in this study [10]. FLC controllers use adaptive decision-making and language reasoning to get around the drawbacks of conventional techniques [11]. Even under fluctuating and unpredictable operating settings, FLC is able to retain precision and stability in temperature management [12] because of its flexibility in

inference and capacity to handle linguistic variations. In addition to enhancing the quality of 3D printed goods, this research helps create more dependable and efficient production line systems by tackling the difficulties associated with accurate temperature management.

2. HARDWARE SYSTEM OF 3D PRINTERS

2.1. Movement Structure

The experimental 3D printer model's core xy is its moving mechanism (Fig. 1(a)). The work area should measure roughly 300mm in length, 300mm in width, and 300mm in height with this design, providing ample room for intricate printing tasks.

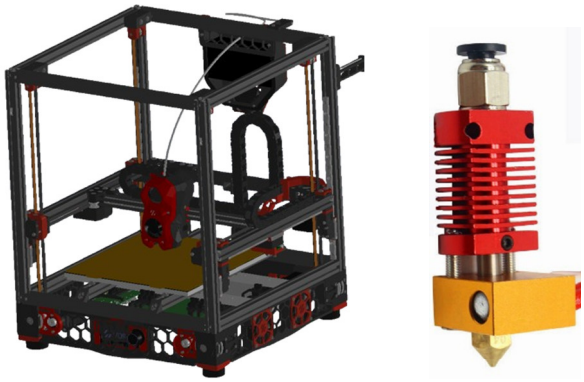

(a) (b)

Fig. 1. Moving mechanism (a) and printhead assembly (b)

2.2. Nozzle Heater Block Model

An aluminum mounting block and a high-power heating element, usually 40W or 50W, rated to run at 24V make up the heating block of the burner in the CoreXY Voron 2.4 3D printer. Like the heating table, this heating element's power dissipation is controlled by varying the duty cycle of the microcontroller's applied PWM (pulse width modulation) signal.

The power supply is controlled by N-channel boost-mode MOSFETs in the developed control system since the heating element requires 24VDC electricity. To guarantee secure insulation and supply the proper gate voltage for the MOSFET, MOSFETs IRLB8743 or comparable series are frequently employed in combination with optical isolators. In order to meet the printing needs of materials like PLA, ABS, or nylon, this guarantees that the heating element runs steadily and maintains the proper temperature throughout the printing process.

2.3. Mathematical model of the heating cluster

The dynamic model of the heating assembly consists of the following components:

Heating Cluster Temperature (Nozzle Temperature, T): The temperature at the heating cluster needs to be maintained stable.

Thermal Dynamics (Thermal Dynamics): Reflects the accumulation and loss of heat through heat transfer processes.

Heating capacity $(Q_{heating})$: Power supplied from the heating element to maintain the printhead temperature.

Heat Loss: Includes heat loss through conductors(k_{base}), convection (h_{conv}), and radiation $(Q_{radiation})$.

Heat Potential of Filament (L_f): The heat required to transfer the filament from a solid to a liquid state.

Line Filament Mass $(\dot{m})$: The amount of filament is pushed through the print head, which affects the heat absorption.

Thermodynamic of Filament(c_f): Specific heat capacity of filament.

A calorific equilibrium equation must be established at the print head in order to create the dynamic model.

Califice Balance.

When the total heat from heating is subtracted from the total heat lost through heat transfer and heat transfer processes, the heat that accumulates in the heating cluster is equal.

Heat Loss (Q_{loss}).

Heat loss through conduction, convection, and radiation is represented as follows:

$$Q_{loss} = k_{base}(T - T_{ambient}) + h_{conv} A_{nozzle}(T - T_{ambient}) + Q_{radiation} \quad (1)$$

In which:

k_{base}: Heat loss coefficient through conduction.

h_{conv}: Convection heat transfer coefficient.

A_{nozzle}: The surface area of the print head.

$T_{ambient}$: Ambient temperature.

$Q_{radiation} = \epsilon\sigma A_{nozzle}(T^4 - T_{ambient}^4)$: Heat lost through radiation, with ϵ is the emissivity coefficient and σ is the Stefan-Boltzmann constant.

Heat Expenditure for Fusing Filament (Q_{melt}).

$$Q_{melt} = \dot{m}(c_f(T - T_f) + L_f) \quad (2)$$

In which:

$\dot{m}$: Filament mass line.

c_f: Specific heat capacity of filament.

T_f: Filament temperature before melting.

L_f: The latent heat of the filament.

Thermal Equilibrium Equation.

Combining the above expressions, the calorific equilibrium equation becomes:

$$C_{therm}\frac{dT}{dt} = Q_{heating} - \begin{bmatrix} k_{base}(T - T_{ambient}) \\ +h_{conv}A_{nozzle}(T - T_{ambient}) \\ +\epsilon\sigma A_{nozzle}(T^4 - T_{ambient}^4) \end{bmatrix} \quad (3)$$

Deduction and Model Simplification.

When nonlinear components, like radiation, do not significantly affect the system, the model can be linearized or reduced for simplicity of control and simulation. Assume $Q_{radiation}$ insignificant, the equation becomes:

$$C_{therm}\frac{dT}{dt} = Q_{heating} - k_{base}(T - T_{ambient}) - h_{conv}A_{nozzle}(T - T_{ambient}) - \dot{m}(c_f(T - T_f) + L_f) \quad (4)$$

Definition of Temperature Error (x).

For the convenience of control, define the temperature error $x = T - T_{ambient}$, then the equation becomes:

$$C_{therm}\frac{dx}{dt} = Q_{heating} - (k_{base} + h_{conv}A_{nozzle})x - \dot{m}(c_f x + L_f) \quad (5)$$

Conversion to Linear Form.

The above equation can be rewritten as:

$$\frac{dx}{dt} = -\frac{(k_{base} + h_{conv}A_{nozzle} + \dot{m}c_f)}{C_{therm}}x + \frac{Q_{heating}}{C_{therm}} - \frac{\dot{m}L_f}{C_{therm}} \quad (6)$$

Call the coefficients:

$$A = -\frac{(k_{base} + h_{conv}A_{nozzle} + \dot{m}c_f)}{C_{therm}} \quad (7)$$

$$B = \frac{1}{C_{therm}} \quad (8)$$

$$C = \frac{-\dot{m}L_f}{C_{therm}} \quad (9)$$

We have:

$$\frac{dx}{dt} = Ax + BQ_{heating} + C \quad (10)$$

2.4. Fuzzy Controller for Heating Assemblies

Controller Output - Input

As the difference between the reference temperature and the actual measured temperature value, the first input variable is regarded as an error:

$$e(k) = T_{ref}(k) - T_{real}(k) \quad (11)$$

With the scaling factor ke, the physical domain of the temperature deviation e(k) is converted to the fuzzy domain of the $e(k)$ deviation. For a 2D fuzzy controller, the second input variable is considered to be the derivative of the deviation, which is directly replaced by the variation of the deviation between two consecutive patterns in order to minimize the effect of the error:

$$\Delta e(k) = \frac{e(k) - e(k-1)}{T_s} \quad (12)$$

The fuzzy domain of the deviation derivative $\Delta e_m(k)$ is created by converting the physical domain of the temperature deviation derivative $\Delta e(k)$ to the ratio factor kec. Fuzzy experience rules are used to infer the fuzzy controller's incremental output from the values of its two input variables, the skew, and its derivatives:

$$\Delta\mu_m(k) = f(e_m(k);\ \Delta e_m(k)) = F(e_m(k)) \quad (13)$$

$$u(k) = u(k-1) + k_u\Delta u_m(k) + k_i e_m(k) \quad (14)$$

In which, f is the fuzzy inference function, FL is its simplified version. With the ku ratio factor, the fuzzy domain of the incremental output $D\mu_m(k)$ is converted to the physical domain.

When applying the Z-transform, the above formulas are reproduced as follows:

$$u(z) = \frac{1}{1 - z^{-1}}\left[k_i e_m(z) + k_u F(e_m(z))\right] \quad (15)$$

The integrator term is the first component in the formula above, while fuzzy incremental input is the second. For summing, the component $\frac{1}{1-z^{-1}}$ is comparable to an integrator in the time domain. Until the e error is zero and there is no longer any stable error, the u control's volume will continue to fluctuate.

Fuzzification and Defuzzification

The process of fuzzification transforms the numerical values of the input variables into fuzzy sets or linguistic variables, and membership functions define how fuzzi a fuzzy set is. This procedure classifies the fuzzy set's members and may be shown via graphical graphs or functions.

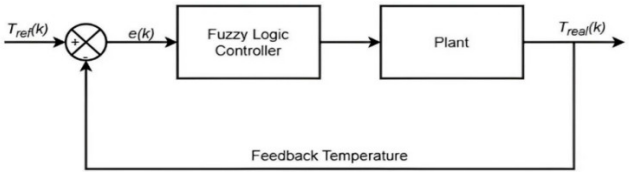

Fig. 2. Block diagram of the fuzzy logic controller

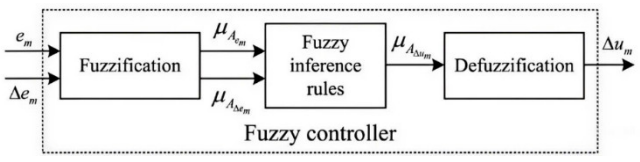

Fig. 3. Block diagram of the fuzzification

Scaling factors and percentage factors are used to allocate the controller's $e_m(k)$, $De_m(k)$, and $D\mu_m(k)$ input variables' fuzzy universe regions to the range [–6.6]. Seven fuzzy subsets are used to explain them: $i = em$, De_m,$D\mu_m$, and Ai = {Negative Big (NB), Negative Medium (NM), Negative Small (NS), Zero (ZO), Positive Small (PS), Positive Medium (PM), and Positive Big (PB)}.

$$\mu_{A_i^{NB}}(x) = \begin{cases} 1 & x \le a_i \\ 1 - 2\left(\frac{x-a_i}{b-a}\right)^2 & a_i \le x \le \frac{a_i+b_i}{2} \\ 2\left(\frac{x-b_i}{b_i-a_i}\right)^2 & \frac{a_i+b_i}{2} \le x \le b_i \\ 0 & x \ge b_i \end{cases} \quad (16)$$

PB (Positive Big): Established based on an S-shaped spline:

$$\mu_{A_i^{PB}}(x) = \begin{cases} 0 & x \le a_i \\ 2\left(\frac{x-b_i}{b_i-a_i}\right)^2 & a_i \le x \le \frac{a_i+b_i}{2} \\ 1 - 2\left(\frac{x-a_i}{b_i-a_i}\right)^2 & \frac{a_i+b_i}{2} \le x \le b_i \\ 1 & x \ge b_i \end{cases} \quad (17)$$

Other fuzzy sets such as NM, NS, ZO, PS, and PM are set up based on a double Gauss function (gauss2 function):

$$\mu_{A_i^j}(x) = \begin{cases} \exp\left[-\frac{\left(x-c1_i^j\right)^2}{2\sigma 1_i^j}\right] & x \le c1_i^j ;\ j = NM, NS, ZO, PS, PM \\ \exp\left[-\frac{\left(x-c2_i^j\right)^2}{2\sigma 2_i^j}\right] & x \ge c2_i^j \end{cases} \quad (18)$$

Functional Characteristics

One significant factor is how the membership functions are shaped. Low-resolution blur sets are applied to significant mistakes, whereas high-resolution blur sets are applied to tiny errors. The controller's precision is enhanced by this heterogeneous distribution.

Defuzzification Process

Applications cannot use blurry results directly; instead, they must be transformed into clear values for additional processing. The centroid approach, which is the most often used defuzzification technique, is represented by the formula:

$$\Delta u_m = \frac{\int x\mu_{A_{Au_m^j}}(x)dx}{\int \mu_{A_{su_m}^j}(x)dx} \quad (19)$$

By transforming the dim inference action into a continuous signal, this procedure modifies the controller's parameter incrementally.

The Legal Basis of the Inference is Fuzzy

The number of fuzzy sets that have been specified for the input variables including all potential combinations and the generation of if-then fuzzy rules using AND and OR inference logic directly influence the size of the rule base (Fig. 4).

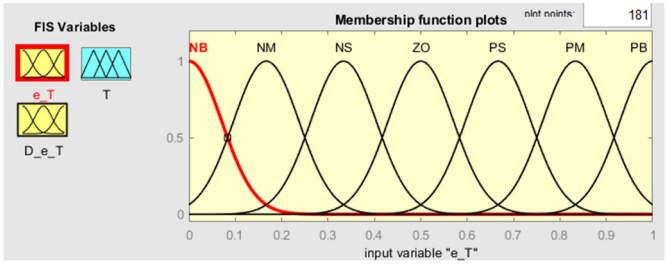

Fig. 4. Graph of results according to fuzzy inference rules

Table 1. 1D fuzzy inference rules

e_m	NB	NM	NS	ZO	PS	PM	PB
D_{u_m}	PB	PM	PS	ZO	NS	NM	NB

Table 2. 2D fuzzy inference rules.

D_{u_m}	e_m							
	NB	NM	NS	NS	PS	PM	PB	NB
D_{e_m}	NB	PB	PB	PM	PM	PM	ZO	ZO
	NM	PB	PB	PM	PS	PS	ZO	NS
	NS	PM	PM	PS	PS	ZO	NS	NS
	ZO	PM	PM	PS	ZO	NS	NM	NM
	PS	PS	PS	ZO	NS	NS	NM	NM
	PM	PS	ZO	NS	NS	NM	NB	NB
	PB	ZO	ZO	NM	NM	NM	NB	NB

The resulting data is shown as a spatial plane as seen in Fig. 5 after the state variables have been configured using the previously discussed rule table.

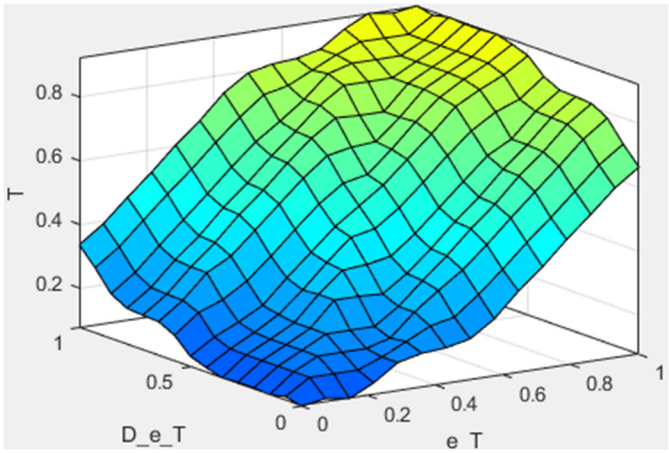

Fig. 5. Fuzzy logic rule surface

3. RESULTS

The simulated temperature response of the controller in both noisy and noise-free scenarios is displayed in the accompanying graph.

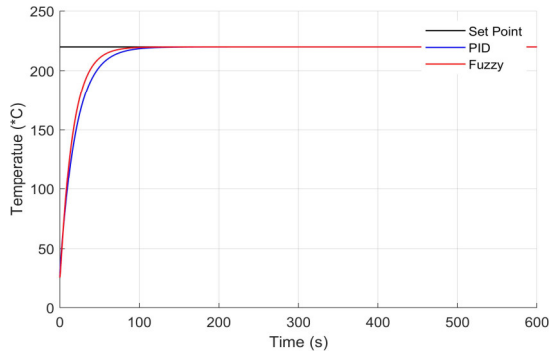

(a)

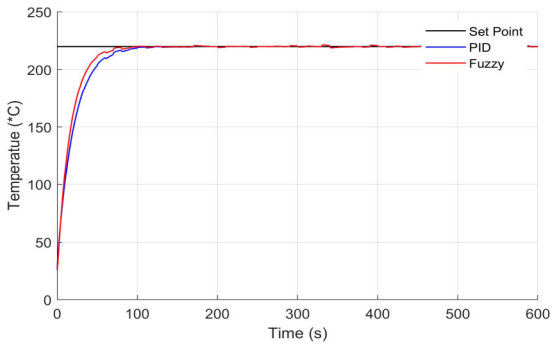

(b)

Fig. 6. System response under noise-free (a) and noisy conditions (b)

The fuzzy logic controller quickly reaches the target temperature and maintains stability with little departure from the set point, as shown by the two graphs in Fig. 6. When disturbances occur, the system maintains its stability and shows better oscillation reduction than the PID controller. This illustrates how the fuzzy controller may lessen the impact of disruptions, guaranteeing precision and stability in applications involving 3D printing.

(a)

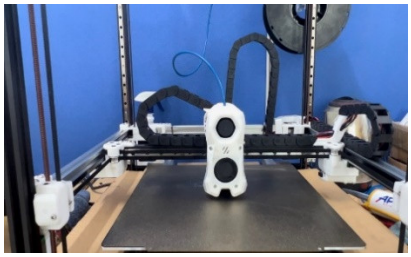

(b)

Fig. 7. Actual operation images of 3D printer (a) and the nozzle heater block (b)

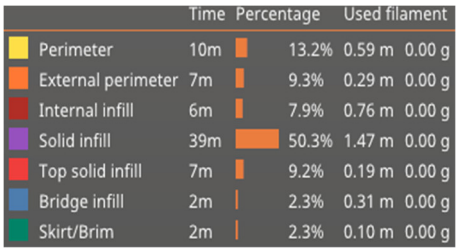

(a)

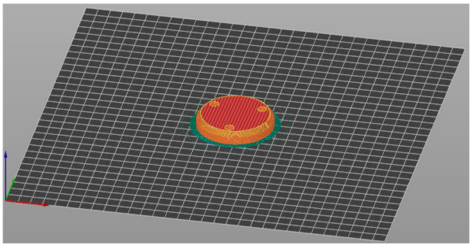

(b)

Fig. 8. Print subject (a) and estimated specifications (b)

The experiments were carried out using a 3D printer that had a fuzzy logic controller installed for controlling the heating block's temperature.

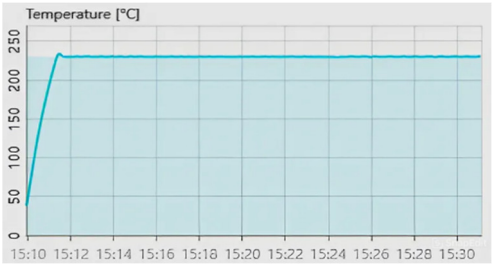

(a)

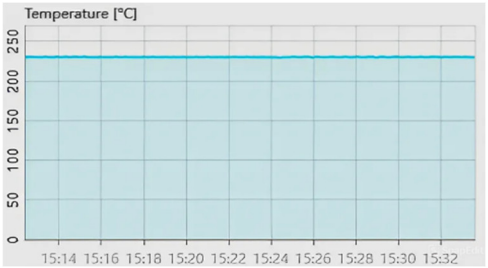

(b)

Fig. 9. Experiment with an output temperature of 215°C. The temperature increases to the set point (a) and maintained at the set point (b)

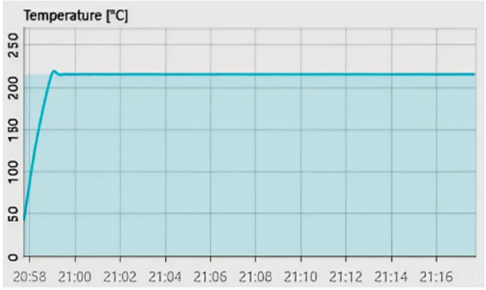

(a)

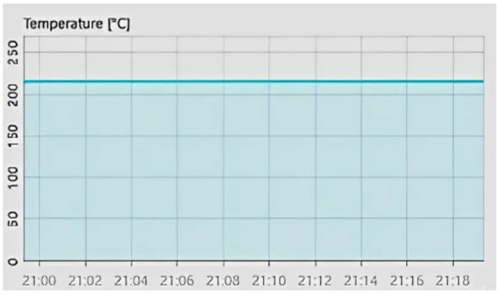

(b)

Fig. 10. Experiment with an output temperature of 230°C. The temperature increases to the set point (a) and maintained at the set point (b)

Following the experiment's findings in Fig. 10 and Fig. 9. The temperature-time graph shows a quick starting rise that takes 1-2 minutes to reach the desired temperature (215°C or 230°C). This outcome shows how well the temperature control algorithm works, guaranteeing a prompt reaction and reducing overshoot.

4. CONCLUSION

According to the approach and data analysis, the traditional controller has a greater peak pass than the fuzzy logic controller, which has a maximum pass of 1%. Thus, the dimming controller performs better than the traditional algorithm. Any industrial application may benefit from the precise control that the fuzzy logic controller's heating system offers. Under all test situations, the controller's reaction fulfills expectations and stays within the necessary maximum and minimum temperatures. It has been demonstrated that fuzzy logic controllers may be used to complete challenging tasks like adaptive setpoint monitoring and heating system noise cancellation. The FLC algorithm may concentrate on many factors, including reaction time, stability error, and peak pass, and it swiftly adjusts to greater time delays while providing a steady response. The controller described in this paper has outstanding durability and tracking speed qualities.

REFERENCES

[1]. A. Lifton V., Lifton G., Simon S., "Options for additive rapid prototyping methods (3D printing) in MEMS technology," *Rapid Prototyping Journal*, 20(5), 403-412, 2014.

[2]. Mikula K., Skrzypczak D., Izydorczyk G., Warchoł J., Moustakas K., Chojnacka K., Witek-Krowiak A., "3D printing filament as a second life of waste plastics - a review," *Environmental Science and Pollution Research*, 28, 12321-12333, 2021.

[3]. Rastogi Prasansha, Gharde Swaroop, Kandasubramanian Balasubramanian, "Thermal effects in 3D printed parts," *3D Printing in Biomedical Engineering*, 43-68, 2020.

[4]. Cui T., Chattaraman V., Sun L., "Examining consumers' perceptions of a 3D printing integrated apparel: a functional, expressive and aesthetic (FEA) perspective," *Journal of Fashion Marketing and Management: An International Journal*, 26(2), 266-2, 2022.

[5]. Ufodike Chukwuzubelu Okenwa, Nzebuka Gaius Chukwuka, "Investigation of thermal evolution and fluid flow in the hot-end of a material extrusion 3D Printer using melting model," *Additive Manufacturing*, 49: 102502, 2022.

[6]. Alsoufi M. S., Alhazmi M. W., Suker D. K., Alghamdi T. A., Sabbagh R. A., Felemban M. A., Bazuhair F. K., "Experimental characterization of the influence of nozzle temperature in FDM 3D printed pure PLA and advanced PLA+," *Am J Mech Eng,* 2019.

[7]. Zolfagharian A., Kaynak A., Bodaghi M., Kouzani A. Z., Gharaie S., Nahavandi S., "Control-based 4D printing: Adaptive 4D-printed systems," *Applied Sciences,* 10(9), 3020, 2020.

[8]. Lee C. C., "Fuzzy logic in control systems: fuzzy logic controller," *IEEE Transactions on systems, man, and cybernetics*, 20(2), 404-418, 1990.

[9]. Tang Hooi Hung, Nur Syazreen Ahmad, "Fuzzy logic approach for controlling uncertain and nonlinear systems: a comprehensive review of applications and advances," *Systems Science & Control Engineering*, 12.1: 2394429, 2024.

[10]. Safaryazdi Alireza, Ali Ghaffari, "APRTC: advanced precise rapid thermal cycling in blow molding by applying fuzzy controller on thermoelectric devices for cooling and heating applications," *Discover Mechanical Engineering*, 3.1: 5, 2024.

[11]. Sathya D., Saravanan G., Thangamani R., "Fuzzy Logic and Its Applications in Mechatronic Control Systems," *Computational Intelligent Techniques in Mechatronics*, 211-241, 2024.

[12]. Gao Z., Trautzsch T. A., Dawson J. G., "A stable self-tuning fuzzy logic control system for industrial temperature regulation," *IEEE Transactions on Industry Applications*, 38(2), 414-424, 2002.